Journal of Power Sources 189 (2009) 543–546

Contents lists available at ScienceDirect

Journal of Power Sources

journal homepage: www.elsevier.com/locate/jpowsour

Short communication

One-dimensional nanostructures as electrode materials for lithium-ion batteries with improved electrochemical performance

Guoxiu Wang*, Xiaoping Shen, Jane Yao

School of Mechanical, Materials and Mechatronic Engineering, Institute for Superconducting and Electronic Materials, University of Wollongong, Wollongong, NSW 2500, Australia

ARTICLE INFO

Article history:
Received 27 July 2008
Received in revised form 8 October 2008
Accepted 10 October 2008
Available online 21 October 2008

Keywords:
One-dimensional nanostructure
Cathode material
Anode material
Lithium-ion battery
Electrochemical performance

ABSTRACT

One-dimensional (1D) nanosize electrode materials of lithium iron phosphate ($LiFePO_4$) nanowires and Co_3O_4–carbon nanotube composites were synthesized by the hydrothermal method. The as-prepared 1D nanostructures were structurally characterized by X-ray diffraction, scanning electron microscopy, and transmission electron microscopy. We tested the electrochemical properties of $LiFePO_4$ nanowires as cathode and Co_3O_4–carbon nanotubes as anode in lithium-ion cells, via cyclic voltammetry and galvanostatic charge/discharge cycling. $LiFePO_4$ nanorod cathode demonstrated a stable performance over 70 cycles, with a remained specific capacity of 140 mAh g^{-1}. Nanocrystalline Co_3O_4–carbon nanotube composite anode exhibited a reversible lithium storage capacity of 510 mAh g^{-1} over 50 cycles. 1D nanostructured electrode materials showed strong potential for lithium-ion batteries due to their good electrochemical performance.

1. Introduction

Lithium-ion batteries are the state-of-the-art and dominant power sources for portable electronic devices. They are also the most promising candidate for electric vehicles, hybrid electric vehicles and energy storage of wind/solar power. Electrode materials (cathode and anode) play a pivotal role in the development of new generation lithium-ion batteries with high energy density. In recent years, huge efforts have been made to develop new electrode materials for lithium-ion batteries with improved electrochemical properties [1–5].

One-dimensional nanostructures, including nanowires, nanorods, nanotubes and nanoribbons, have been extensively investigated for applications in the areas of nanoscale electronic and photonic devices, chemical and biological sensors, and energy storage and conversion [6–10]. V_2O_5 nanotubes and nanowires of $LiCoO_2$ and $Li(Ni_{1/2}Mn_{1/2})O_2$ have been prepared and have exhibited interesting electrochemical performance [11–13]. Cobalt oxide (Co_3O_4) nanowires and gold–cobalt oxide hybrid nanowires were synthesized by using a virus-enabled synthesis process. Those cobalt oxide nanowires demonstrated a stable capacity of 800–1200 mAh g^{-1} [14]. Porous Co_3O_4 nanotubes were prepared using carbon nanotubes (CNTs) as templates, and these demonstrated a high capacity of 1200 mAh g^{-1} and good cycle life [15]. Tin oxide (SnO_2) nanowires were prepared through a self-catalysis-grown process via thermal evaporation. SnO_2 nanowires showed better electrochemical performance than that of microcrystalline SnO_2 powders due to the increased charge-transfer properties along the radial direction of the nanowire [16]. Nanocrystalline SnSb–carbon nanotube composite anode materials were synthesized by means of reductive precipitation. The SnSb–CNTs nanocomposite delivered an enhanced reversible capacity and stable cyclic retention [17].

In this paper, we report the hydrothermal synthesis of lithium iron phosphate nanowires as a cathode material and nanocrystalline Co_3O_4–carbon nanotubes as an anode material for lithium-ion batteries. The electrochemical properties of the as-prepared 1D nanostructured materials were systematically tested. The improved electrochemical performance of these 1D nanostructures as electrode materials in lithium-ion cells could be ascribed to the facile lithium diffusion and high electrochemical reactivity.

2. Experimental

All reagents were analytical grade and purchased from Sigma–Aldrich. In a typical synthesis process for preparing $LiFePO_4$ nanowires, 1.5 mmol ferrous sulfate ($FeSO_4{\cdot}7H_2O$), 1.5 mmol ammonium dihydrogen phosphate ($NH_4{\cdot}H_2PO_4$) and 3 mmol lithium hydroxide (LiOH) were dissolved in 8 ml de-ionized water. After stirring, 0.3 g nitrilotriacetic acid (NTA) surfactant and 7 ml

* Corresponding author. Fax: +61 2 42215731.
E-mail address: gwang@uow.edu.au (G. Wang).

0378-7753/$ – see front matter © 2008 Elsevier B.V. All rights reserved.
doi:10.1016/j.jpowsour.2008.10.044

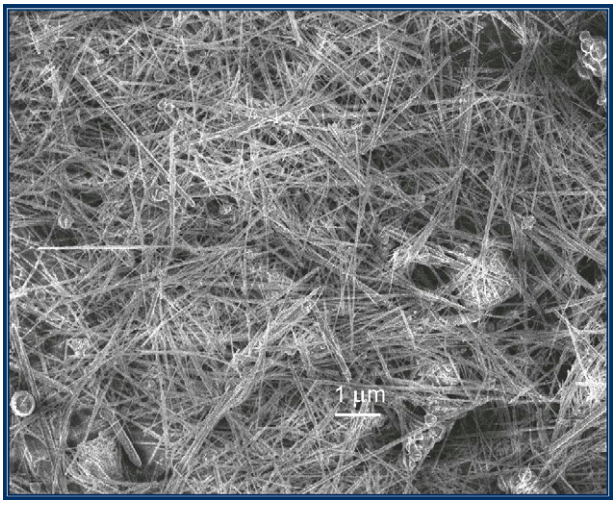

Fig. 1. SEM image of $LiFePO_4$ nanowires.

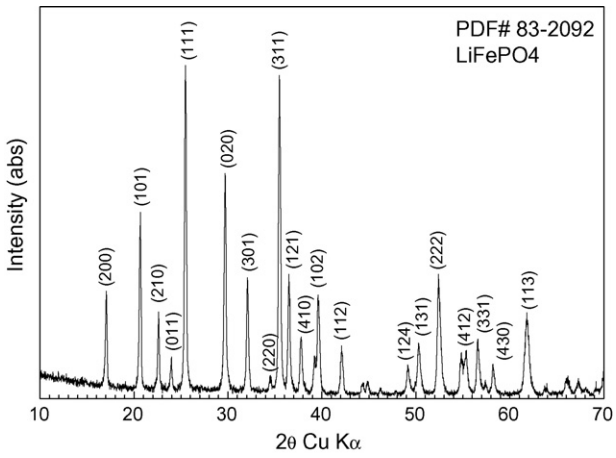

Fig. 2. X-ray diffraction pattern of the as-prepared $LiFePO_4$ nanowires.

isopropanol were added and the pH value of the mixture was adjusted to 9 by adding concentrated ammonia. The mixed solution was then transferred into a 25-ml stainless steel Teflon-lined autoclave. The autoclave was sealed, kept at 180–220 °C for 20 h, and then naturally cooled to room temperature. After the hydrothermal reaction, the solution was centrifuged and washed with distilled water a number of times. The product was dried at 60 °C in a vacuum oven for 4 h. Nanocrystalline Co_3O_4–CNTs composites were also synthesized by a hydrothermal process. 0.25 g $Co(CH_3COO)_2{\cdot}4H_2O$ was dissolved in 10 ml de-ionized water. 15 mg multiwalled carbon nanotubes were dispersed in the solution by ultrasonication. The pH value was adjusted by dropwise addition of 1.3 ml concentrated ammonia solution. The mixture was transferred into a 20-ml autoclave, sealed, and maintained at 150 °C for 5 h. The resulting black products were separated by centrifugation, washed with distilled water, and dried in vacuum at 60 °C for 5 h.

The prepared samples were characterized by X-ray diffraction (XRD, Cu Kα radiation, Philips 1730), scanning electron microscopy (SEM, JEOL JSM 6460A) and transmission electron microscopy (TEM, JEOL 2011). The electrochemical evaluation of $LiFePO_4$ nanowires and nanocrystalline Co_3O_4–CNTs was accomplished by assembling CR2032 coin cells. The electrodes were made by dispersing 82 wt% active materials, 8 wt% polyvinylidene fluoride (PVDF) binder and 8 wt% carbon black in *n*-methyl pyrolidone (NMP) solvent to form a homogeneous slurry. The slurries were uniformly pasted on Al foil ($LiFePO_4$ nanowire sample) and Cu foil (Co_3O_4–CNTs sample). These prepared electrode sheets were dried at 120 °C in a vacuum oven for 12 h and pressed under a pressure of approximately 200 kg cm^{-2}. The electrolyte was 1 M $LiPF_6$ in a 1:1 mixture of ethylene carbonate and dimethyl carbonate. Li metal foil was used as the counter and reference electrode. The cells were galvanostatically charged and discharged at a current density of 0.1 C. The cyclic voltammetry (CV) curves were measured at 0.1 mV s^{-1}.

3. Results and discussion

Fig. 1 shows an SEM image of the as-prepared $LiFePO_4$ nanowires. The nanowires have a diameters in the range of a few hundred nanometers and a lengths extending a few tens of micrometers. We noted that a small amount of $LiFePO_4$ powders was also present. However, most of the products are nanowires, indicating that our hydrothermal process can be effectively applied to synthesize $LiFePO_4$ nanowires. The phase purity of the as-synthesized $LiFePO_4$ nanowires was analyzed by X-ray diffraction. Fig. 2 shows the XRD pattern of the $LiFePO_4$ nanowires. All diffraction lines are indexed to the orthorhombic crystal structure (space group: *pnma*, triphylite) [18]. No any impurity phase was detected by XRD. The electrochemical reactivity of $LiFePO_4$ nanowires was evaluated by cyclic voltammetry. Fig. 3 shows a typical cyclic voltammograms (CVs) of $LiFePO_4$ nanowires as cathode in lithium-ion cells. The $LiFePO_4$ nanowire cathode displays a reduction peak at 3.34 V and an oxidation peak at 3.52 V vs. the Li/Li^+ reference electrode. After 50 scanning cycle, the intensity and shape of the redox peaks for $LiFePO_4$ nanowire cathode do not decrease or change very much, indicating good reversibility of lithium insertion and extraction in the nanowire host. The specific capacity and cyclability of the $LiFePO_4$ cathode were further tested by constant current charge/discharge cycling. Fig. 4 shows the charge/discharge voltage profiles of $LiFePO_4$ nanowire cathode. The cell was charged and discharged at the rate of 0.1 C in the voltage range of 2.75–4.20 V. $LiFePO_4$ nanowire cathode exhibited a flat charge plateau at 3.51 V and a flat discharge plateau at 3.33 V, which match the redox peaks in the CV curve very well. The cyclability of $LiFePO_4$ nanowire cathode is shown as the inset in Fig. 4. The initial discharge capacity for $LiFePO_4$ nanowire cathode reached about 150 mAh g^{-1}. After 60 cycles, the electrode still maintained a specific capacity of 138 mAh g^{-1}, which shows an improved cyclability than that of uncoated and undoped $LiFePO_4$ powders reported previously [18]. There is no carbon coating on the surface of the $LiFePO_4$ nanowires.

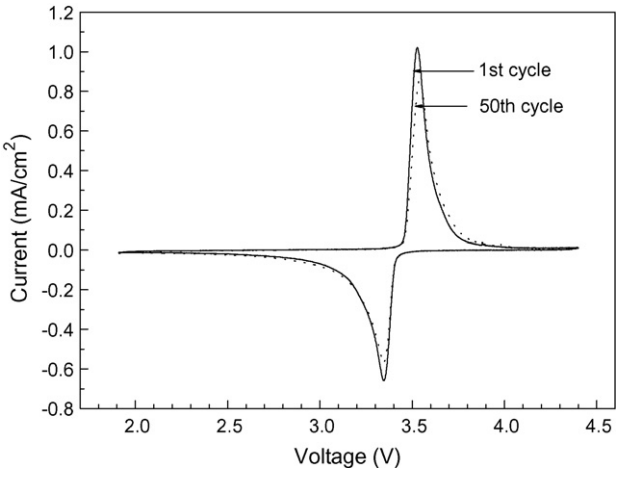

Fig. 3. Cyclic voltammograms of $LiFePO_4$ nanowires as cathode in lithium-ion cell. The scanning rate was 0.1 mV s^{-1}.

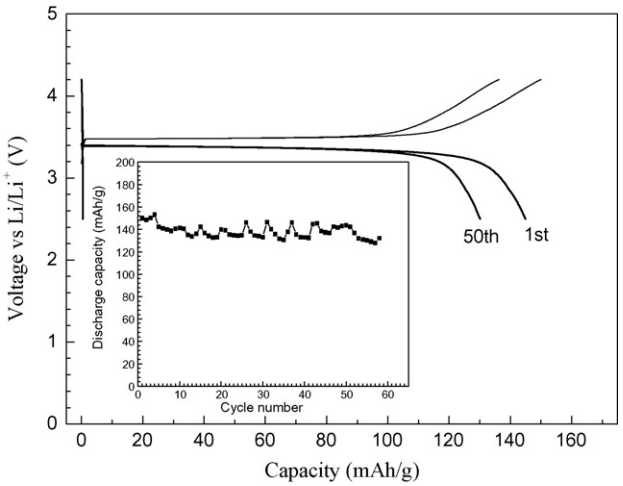

Fig. 4. Galvanostatic voltage profiles of $LiFePO_4$ nanowire cathode in lithium-ion cells. The inset shows discharge capacity vs. cycle number.

The good electrochemical performance of $LiFePO_4$ nanowires as cathode in lithium-ion cells could be attributed to the fact that the 1D nanowires provide a short path for lithium diffusion.

Fig. 5 shows the X-ray diffraction pattern of Co_3O_4–CNTs composites. All diffraction peaks can be indexed to the cubic Co_3O_4 phase (JCPDS no. 42-1467). The lattice constant (a) was calculated to be $a = 8.079$ Å. The XRD pattern of Co_3O_4–CNTs composites confirms the formation of crystalline Co_3O_4 through the hydrothermal synthesis process. The morphology of Co_3O_4–CNTs was observed by TEM analysis. A low magnification TEM image of the as-prepared Co_3O_4–CNTs is presented in Fig. 6(a). In general, the surfaces of the carbon nanotubes are covered by Co_3O_4 nanocrystals. The individual Co_3O_4 nanocrystals have a size in the range of 20 nm. The lattice resolved high resolution TEM image of Co_3O_4 nanocrystals is shown in Fig. 6(b), which further confirmed the crystalline nature of those Co_3O_4 nanocrystals. The weight percentage of Co_3O_4 in the Co_3O_4–CNTs composite was determined by thermogravimetric analysis. The composite consisted of 80 wt% Co_3O_4 and 20 wt% carbon nanotubes. Both Co_3O_4 and carbon nanotubes have lithium storage capability. The reaction between Co_3O_4 and lithium ions follows a conversion reaction mechanism, accompanied by substantial volume change [3,19]. On the other hand, lithium ions can reversibly intercalate and de-intercalate in carbon nanotubes [20]. Therefore, by combining Co_3O_4 and CNTs with their one-dimensional nanostructure, it is possible to achieve good electrochemical performance for Co_3O_4–CNTs composite with the configuration of nanosize Co_3O_4 crystals deposited on a carbon nanotube matrix. The electrochemical properties of Co_3O_4–CNTs composite anodes were tested by galvanostatic charge/discharge cycling. Fig. 7 shows the charge/discharge voltage profiles of Co_3O_4–CNTs as anode in the first and the second cycle. The Co_3O_4–CNTs nanocomposite exhibited an initial lithium storage capacity of 1252 mAh g^{-1} and an irreversible capacity of 412 mAh g^{-1} in the first cycle. This irreversible capacity may originate from the formation of the surface–electrolyte-interface layer and the insertion of lithium ions into the cavities of CNTs. The discharge capacity (lithium storage) of Co_3O_4–CNTs was gradually stabilized from the second cycle. The cycling performance of Co_3O_4–CNTs is further shown in Fig. 8, in which stable cycling performance has been demonstrated for Co_3O_4–CNTs anode. After 50 cycles, the Co_3O_4–CNTs anode still delivers a specific capacity of 510 mAh g^{-1}. This could be attributed to the buffer effect provided by the carbon nanotube matrix, which cushions the volume change during the lithiation and de-lithiation process. The Co_3O_4–CNTs anodes exhibit a significantly improved electrochemical performance, compared to Co_3O_4 anodes [21] and CNTs anodes [22].

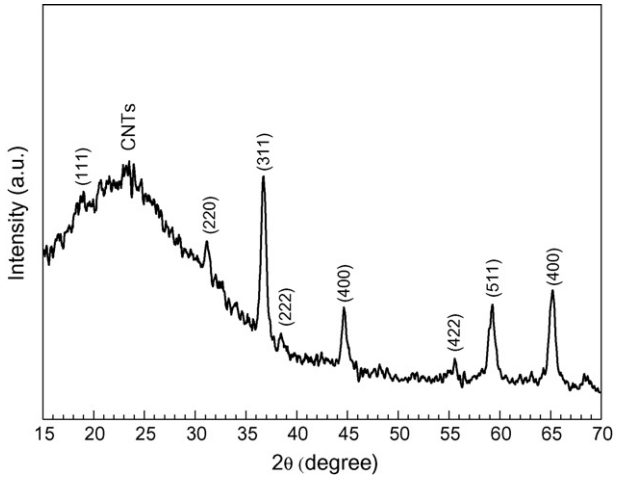

Fig. 5. X-ray diffraction pattern of nanocrystalline Co_3O_4–carbon nanotube composite.

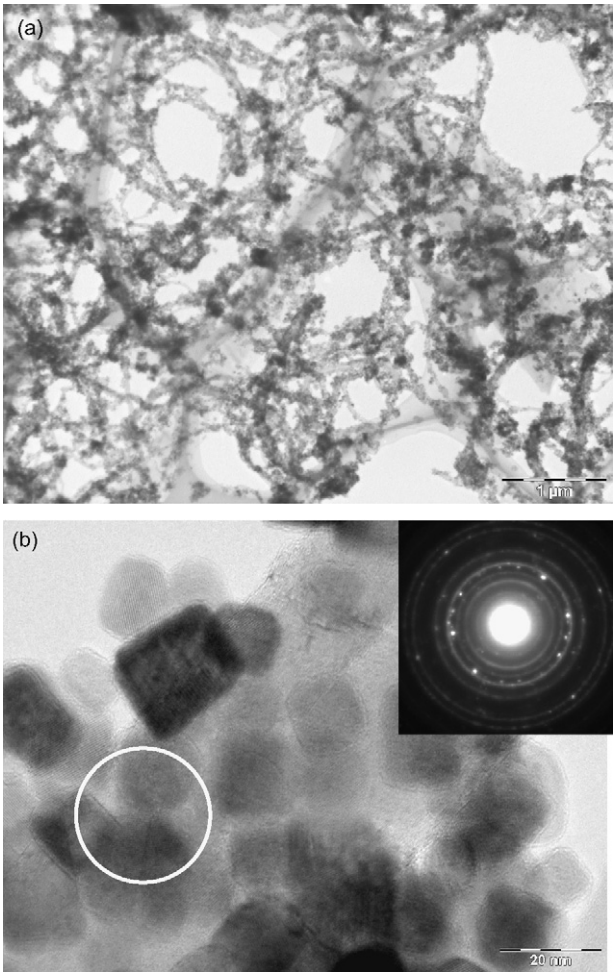

Fig. 6. (a) Low magnification TEM image of nanocrystalline Co_3O_4–carbon nanotube composite, showing the deposition of Co_3O_4 nanocrystals on the carbon nanotube matrix. (b) High resolution TEM image of Co_3O_4–CNTs, from which the lattice of Co_3O_4 can be resolved. The inset is the selected electron diffraction pattern corresponding to the region marked with the white circle.

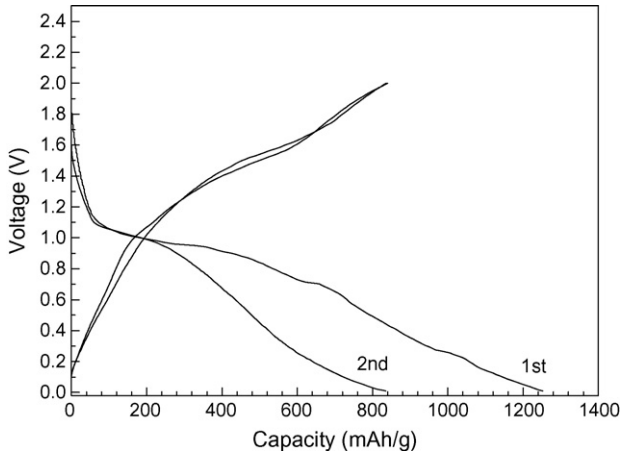

Fig. 7. The charge/discharge voltage profiles of nanocrystalline Co_3O_4–carbon nanotube composites as anode in lithium-ion cell.

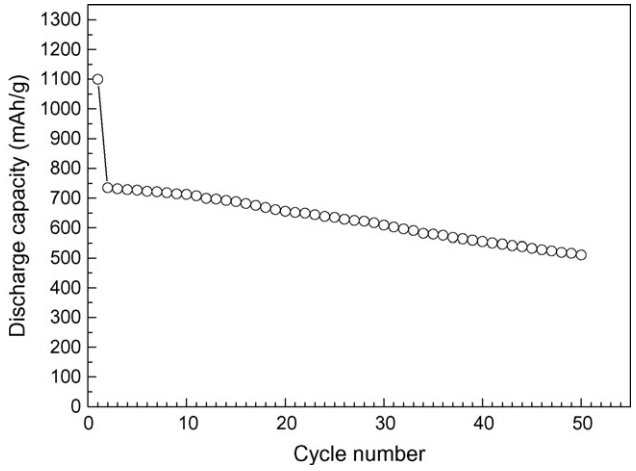

Fig. 8. Discharge capacity vs. cycle number for nanocrystalline Co_3O_4–carbon nanotube composite as anode in lithium-ion cell.

4. Conclusions

We have successfully prepared lithium iron phosphate nanowires and nanocrystalline Co_3O_4–carbon nanotubes composites via a hydrothermal synthesis process. The cathode composed of $LiFePO_4$ nanowires without carbon coating exhibited a specific capacity of 140 mAh g^{-1}. When used as anode materials in lithium-ion cells, nanosize Co_3O_4–carbon nanotube composite anode can maintain a reversible lithium storage capacity of 510 mAh g^{-1} over 50 cycles. Controllable synthesis of one-dimensional nanostructures could be further explored to improve the performance of lithium-ion batteries.

Acknowledgement

We are grateful for the financial support from the Australian Research Council (ARC) through the ARC Discovery project (DP0772999).

References

[1] J.-M. Tarascon, M. Armand, Nature 414 (2001) 359.
[2] K. Kang, Y.S. Meng, J. Bréger, C.P. Grey, G. Ceder, Science 311 (2006) 977.
[3] P. Poizot, S. Laruelle, S. Grugeon, L. Dupont, J.-M. Tarascon, Nature 407 (2000) 496.
[4] M.S. Whittingham, Chem. Rev. 104 (2004) 4271.
[5] H. Liu, G.X. Wang, Electrochem. Commun. 10 (2008) 243.
[6] X.F. Duan, Y. Huang, Y. Cui, J.F. Wang, C.M. Lieber, Nature 409 (2001) 66.
[7] Y. Huang, X.F. Duan, Y. Cui, C.M. Lieber, Nano Lett. 2 (2002) 101.
[8] G.X. Wang, J.S. Park, D. Wexler, M.S. Park, J.H. Ahn, Inorg. Chem. 46 (2007) 4778.
[9] M. Law, L.E. Greene, J.C. Johnson, R. Saykally, P.D. Yang, Nat. Mater. 4 (2005) 455.
[10] L. Vayssieres, Adv. Mater. 15 (2003) 464.
[11] S. Nordlinder, L. Nyholm, T. Gustafsson, K. Edstrom, Chem. Mater. 18 (2006) 495.
[12] F. Jiao, K.M. Shaju, P.G. Bruce, Angew. Chem. Int. Ed. 44 (2005) 6550.
[13] Y.K. Zhou, H.L. Li, J. Mater. Chem. 12 (2002) 681.
[14] K.T. Nam, D.W. Kim, P.J. Yoo, C.Y. Chiang, N. Meethong, P.T. Hammond, Y.M. Chiang, A.M. Belcher, Science 312 (2006) 885.
[15] N. Du, H. Zhang, B. Chen, J.B. Wu, X.Y. Ma, Z.H. Liu, Y.Q. Zhang, D. Yang, X.H. Huang, J.P. Tu, Adv. Mater. 19 (2007) 4505.
[16] M.S. Park, G.X. Wang, Y.M. Kang, D. Wexler, S.X. Dou, H.K. Liu, Angew. Chem. Int. Ed. 46 (2007) 750.
[17] M.S. Park, S.A. Needham, G.X. Wang, Y.M. Kang, J.S. Park, S.X. Dou, H.K. Liu, Chem. Mater. 19 (2007) 2406.
[18] S.Y. Chung, J.T. Bloking, Y.M. Chiang, Nat. Mater. 2 (2002) 123.
[19] V. Pralong, D.C.S. Souza, K.T. Leung, L. Nazar, Electrochem. Commun. 4 (2002) 516.
[20] W.X. Chen, J.Y. Lee, Z. Liu, Electrochem. Commun. 4 (2002) 260.
[21] G.X. Wang, Y. Chen, K. Konstantinov, J. Yao, J.H. Ahn, H.K. Liu, S.X. Dou, J. Alloys Compd. 340 (2002) L5.
[22] G.X. Wang, J.H. Ahn, J. Yao, M. Lindsay, H.K. Liu, S.X. Dou, J. Power Sources 119–121 (2003) 16.